

Schisandrin B inhibits epithelial-mesenchymal transition and stemness of large-cell lung cancer cells and tumorigenesis in xenografts via inhibiting the NF- κ B and p38 MAPK signaling pathways

SHUPING LI¹, HONG WANG¹, RUIDONG MA¹ and LI WANG²

Departments of ¹Thoracic and Cardiac Surgery, and ²Anesthesiology,
The First Affiliated Hospital of Chengdu Medical College, Chengdu, Sichuan 610500, P.R. China

Received August 24, 2020; Accepted January 29, 2021

DOI: 10.3892/or.2021.8066

Abstract. Lung cancer is one of the most common types of cancer in the world, resulting in numerous cancer-associated deaths. The properties of cancer stem cells (CSCs) are important for the initiation and deterioration of lung cancer. Schisandrin B (SchB), an active compound extracted from *Schisandra chinensis*, exerts anticancer effects in various malignancies, including lung cancer. Nevertheless, the potential of SchB in epithelial-mesenchymal transition (EMT) and CSC features of large-cell lung cancer remains unclear. The present study established cancer stem-like cells derived from large-cell lung cancer cells, NCI-H460 and H661, and revealed that SchB inhibited the viability of cancer stem-like cells at concentrations of $\geq 40 \mu\text{mol/l}$. Moreover, SchB prominently inhibited cell migration, invasion and EMT. Sphere-forming assays and western blotting demonstrated that the stemness of cancer stem-like cells was alleviated by SchB treatment. Mechanistically, the current findings revealed that SchB contributed to the suppression of the NF- κ B and p38 MAPK signaling pathways. Notably, further results revealed that the malignant behaviors of NCI-H460-CSCs induced by the activation of the NF- κ B and p38 MAPK signaling pathways were suppressed by SchB treatment. Consistently, the inhibitory role of SchB in EMT and CSC activities, as well as in the activation of the NF- κ B and p38 MAPK signaling

pathways, was confirmed *in vivo*. In conclusion, the present study demonstrated that SchB exerted inhibitory effects on large-cell lung cancer cells via targeting the NF- κ B and p38 MAPK signaling pathways, suggesting that SchB may act as a potential therapeutic drug for large-cell lung cancer.

Introduction

Lung cancer is regarded as one of the leading causes of cancer-associated mortality worldwide, accounting for ~18.4% of cancer-associated deaths (1,2). The 5-year survival rate of patients with lung cancer is low (range, 4-17%) due to the malignant characteristics of early metastasis and relapse (3,4). Although increasing progress in a variety of therapeutic interventions, such as chemotherapy, radiotherapy and targeted drugs, the prognosis of patients with lung cancer remains unsatisfactory due to the limited efficacy of clinical therapies resulting from drug resistance and adverse effects (5). Thus, it is indispensable to identify novel therapeutics for the treatment of lung cancer.

Cancer stem cells (CSCs) are well-known heterogeneous tumor cells characterized by the capacity to self-renew, indefinitely proliferate, differentiate and initiate tumors; these properties are considered as the promoting factors for tumorigenesis, metastasis and recurrence (6-8). CSCs were first discovered in acute leukemia and they serve a critical role in a wide spectrum of malignancies, including breast, ovarian, cervical and lung cancer (9-14). Since the characteristics of stemness are implicated in the development of lung cancer, eliminating CSC properties may be a potentially effective therapeutic strategy for lung cancer.

It is widely acknowledged that epithelial-mesenchymal transition (EMT) is defined as a cellular programme with representative changes of cell phenotype from an epithelial to a mesenchymal morphology, which is strongly associated with the acquisition of CSC properties (15). Multiple studies have demonstrated that EMT is of great importance in the initiation and evolution of tumors, since it confers a fortified potential for carcinogenesis and metastasis, and enhances the resistance to chemotherapeutic agents (16,17). Since there is a tight association between EMT induction and the gain of cancer

Correspondence to: Professor Li Wang, Department of Anesthesiology, The First Affiliated Hospital of Chengdu Medical College, 278 Middle Baoguang Avenue, Xindu, Chengdu, Sichuan 610500, P.R. China
E-mail: wanglicdmc@126.com

Abbreviations: CCK-8, Cell Counting Kit-8; CSC, cancer stem cell; EMT, epithelial-mesenchymal transition; RIPA, radioimmunoprecipitation; IHC, immunohistochemical; SchB, Schisandrin B

Key words: SchB, large-cell lung cancer, EMT, stemness, NF- κ B, p38 MAPK

stem-like traits (18), the role of EMT in the maintenance of CSC signatures is largely to be explored.

Schisandrin B (SchB) is the most active dibenzocyclooctadiene derivative extracted from the traditional Chinese herb *Schisandra chinensis*, which is clinically used for the treatment of cardiovascular diseases in China, as well as viral and chemical hepatitis (19). Increasing studies have demonstrated that SchB possesses diverse pharmacological effects, including antioxidant, anti-asthma, anti-inflammation and especially anticancer effects (20,21). For example, SchB inhibits STAT3 to exert potent antitumor activity in triple-negative breast cancer (22). SchB suppresses glioma cell proliferation and invasion via regulation of the HOTAIR-microRNA-125a-mTOR signaling pathway (23). For lung cancer, SchB hinders the proliferation of lung adenocarcinoma A549 cells via promoting cell cycle arrest and apoptosis (24). Additionally, TGF- β 1-induced EMT in human A549 cells is suppressed by SchB (25). However, the function of SchB in EMT and CSC traits of large-cell lung cancer cells remains unclear. Therefore, the present study aimed to clarify the effects of SchB on the tumorigenesis of large-cell lung cancer and the latent molecular mechanism involved in the potential of SchB.

Materials and methods

Plant material. SchB extracted from *Schisandra chinensis* was purchased from Sigma-Aldrich (Merck KGaA; cat. no. PHL89786). The purity of SchB was >95%.

Cell culture and treatment. Human large-cell lung cancer cell lines, NCI-H460 and H661, were supplied by the American Type Culture Collection. Cells were grown in RPMI-1640 medium containing 10% FBS (both HyClone; Cytiva) under an atmosphere of 5% CO₂ in a sterile incubator at 37°C.

To establish cancer stem-like cells (named NCI-H460-CSC or H661-CSC), NCI-H460 or H661 cells were maintained for 10 days at 37°C in serum-free DMEM/F12 medium (Sigma-Aldrich; Merck KGaA) complemented with 100 μ g/ml insulin (Sigma-Aldrich; Merck KGaA), 20 ng/ml epidermal growth factor (Invitrogen; Thermo Fisher Scientific, Inc.), 20 ng/ml basic fibroblast growth factor (Invitrogen; Thermo Fisher Scientific, Inc.), 5 mM Hepes (Sigma-Aldrich; Merck KGaA), 0.6% glucose (Sigma-Aldrich; Merck KGaA) and 0.4% BSA (Sigma-Aldrich; Merck KGaA). The media was changed every 2 days. CD133⁺ cells (cancer stem-like cells) in induced cells were isolated by magnetic-activated cell sorting for further experiments. According to the manufacturer's instructions, cells were labeled using CD133-PE antibody (Miltenyi Biotec GmbH; 1:50; cat. no. 130-113-748) at 4°C for 10 min in the dark and underwent magnetic sorting with the help of 10 μ l anti-PE Multisort MicroBeads (Miltenyi Biotec GmbH; cat. no. 130-090-757) per 90 μ l cell suspension. Flow cytometry was used to analyze CD133⁺ cells. In subsequent experiments, sorted cells (cancer stem-like cells) were incubated in serum-free DMEM/F12 medium containing the aforementioned growth factors.

TNF- α and anisomycin were supplied by R&D Systems and Invitrogen (Thermo Fisher Scientific, Inc.), respectively. To activate the NF- κ B and MAPK signaling pathways, cells were incubated with 10 ng/ml TNF- α and 2 ng/ml anisomycin

for 30 min at 37°C, respectively. For cells treated with SchB and TNF- α or anisomycin, cells were treated with 40 μ mol/l SchB for 12 h at 37°C and then stimulated with 10 ng/ml TNF- α or 2 ng/ml anisomycin for 30 min at 37°C.

Cell Counting Kit-8 (CCK-8) assay. Cancer stem-like cells and parental cells were inoculated into 96-well plates at a density of 10³ cells/well and cultured at 37°C. After reaching 80% confluence, cancer stem-like cells and parental cells were incubated with different doses of SchB (0, 5, 10, 20, 40, 80, 120 and 160 μ mol/l) at 37°C. After 72 h of treatment with SchB, 10 μ l CCK-8 reagent (MedChemExpress) was added for 2 h at 37°C. Subsequently, the optical density value at 450 nm was determined using a microplate reader (Molecular Devices, LLC).

Flow cytometry analysis. Flow cytometry was used to examine the ratio of CD133⁺ cells according to the manufacturer's instructions (BD Biosciences). Following different treatments, the collected CSCs were rinsed with PBS, followed by incubation with a primary antibody against CD133 (Abcam; 1:100; cat. no. ab216323) at room temperature for 30 min and then probed with an Alexa Fluor594-labeled IgG secondary antibody (Abcam; 1:2,000; cat. no. ab150080) at 4°C in the dark for 30 min. The ratio of CD133⁺ cells was analyzed using a BD FACSCalibur™ flow cytometer (BD Biosciences) and FlowJo 7.6 software (FlowJo LLC).

Cell cycle was analyzed via flow cytometry after PI staining. In brief, cancer stem-like cells and parental cells were harvested and washed with PBS twice, followed by fixation using ice-cold 70% ethanol for 1 h at 4°C. Subsequently, cells were stored at -20°C. Before analysis, fixed cells were washed with PBS twice, and incubated in PBS containing 50 μ g/ml PI (Beyotime Institute of Biotechnology), 0.3% Triton-X 100 and 100 μ g/ml RNase A (Sigma-Aldrich; Merck KGaA) in the dark for 30 min at 37°C. Afterwards, ~3x10⁴ events were subjected to flow cytometry analysis using a BD FACSCalibur™ flow cytometer (BD Biosciences), and the percentage of cells at different stages of the cell cycle was analyzed using the FlowJo 7.6 software.

Wound healing assay. Following treatment, 1x10⁵ cancer stem-like cells were seeded in 6-well plates. When reaching 90% confluence, a sterile micropipette tip was used to scrape the cell monolayer to form the wound. Subsequently, the cell monolayer was washed with PBS and cultured with serum-free DMEM/F12 medium containing the aforementioned growth factors at 37°C. The distance of wound gap was monitored and photographed using an inverted light microscope (Nikon Corporation; magnification, x100 and x200) at 0 and 48 h following scratching.

Cell invasion assay. The invasive capacity of CSCs was estimated using Transwell assays with Matrigel-coated Transwell inserts (Corning, Inc.). In brief, after treatment, 5x10⁴ cells were seeded in the upper compartment containing 200 μ l serum-free DMEM/F12 medium containing the aforementioned growth factors, while 600 μ l complete DMEM/F12 medium (containing 10% FBS and the aforementioned growth factors) was added to the lower

compartment. Following 24 h of incubation at 37°C, cells in the upper chamber were removed using a cotton swab. The invaded cells were immobilized in 4% paraformaldehyde at room temperature for 10 min, stained with 0.5% crystal violet at room temperature for 15 min and photographed in five randomly selected fields under an inverted light microscope (Nikon Corporation; magnification, x100 and x200).

Sphere-forming assay. After different treatments, 5×10^3 cancer stem-like cells were inoculated into each well of 6-well ultralow attachment plates (Corning, Inc.) and incubated at 37°C in serum-free DMEM/F12 medium containing the aforementioned growth factors for 10 days. The medium was replaced every other day. Images were obtained with an inverted light microscope (Nikon Corporation; magnification, x400). Spheres that reached a diameter of 100 μm in five random fields were counted for one sample. Each group was replicated three times.

Western blot analysis. Cells were lysed with radioimmunoprecipitation assay (RIPA) buffer (Beyotime Institute of Biotechnology). Tumor tissues were homogenized in RIPA buffer. Protein concentration was determined using a BCA assay kit (Beyotime Institute of Biotechnology). Equal amounts of proteins (50 $\mu\text{g}/\text{lane}$) were electrophoretically separated via 10% SDS-PAGE and transferred to PVDF membranes (EMD Millipore). Subsequently, membranes were blocked with 5% skimmed milk, followed by incubation with primary antibodies overnight at 4°C and then incubation with appropriate HRP-labeled secondary antibodies (Abcam; 1:5,000; cat. nos. ab6721 and ab6728) at room temperature for 1 h. An enhanced chemiluminescence kit (Beyotime Institute of Biotechnology) was used to detect the protein signals. The specific primary antibodies included antibodies against E-cadherin (Abcam; 1:200; cat. no. ab219332), vimentin (Abcam; 1:1,000; cat. no. ab8978), N-cadherin (Abcam; 1:1,000; cat. no. ab245117), CD133 (Abcam; 1:1,000; cat. no. ab216323), CD44 (Abcam; 1:1,000; cat. no. ab243894), octamer-binding transcription factor 4 (Oct-4; Abcam; 1:10,000; cat. no. ab200834), B lymphoma Mo-MLV insertion region 1 homolog (Bmi-1; Abcam; 1:10,000; cat. no. ab126783), inhibitor of nuclear factor κB α (I $\kappa\text{B}\alpha$; Abcam; 1:1,000; cat. no. ab76429), phosphorylated (p)-I $\kappa\text{B}\alpha$ (Abcam; 1:10,000; cat. no. ab133462), p65 (Abcam; 1:5,000; cat. no. ab32536), p-p65 (Abcam; 1:1,000; cat. no. ab76302), JNK (Cell Signaling Technology, Inc; 1:1,000; cat. no. 9252), p-JNK (Cell Signaling Technology, Inc. 1:1,000; cat. no. 9251), p38 (Cell Signaling Technology, Inc.; 1:1,000; cat. no. 212), p-p38 (Cell Signaling Technology, Inc; 1:1,000; cat. no. 9216), MEK (Cell Signaling Technology, Inc.; 1:1,000; cat. no. 4694), p-MEK (Cell Signaling Technology, Inc.; 1:1,000; cat. no. 9154) and GAPDH (Abcam; 1:5,000; cat. no. ab8245). GAPDH served as the loading control. ImageJ software (v1.5; National Institutes of Health) was used for densitometry analysis.

Xenograft tumors. All experimental procedures performed in the present study were approved by the Ethics Committee of the First Affiliated Hospital of Chengdu Medical College (Chengdu, China). A total of 30 male 6-week-old nude mice (weight, 18–22 g) were purchased from Chengdu Dashuo Laboratory Animal Co., Ltd. Mice were maintained in

pathogen-free devices under a controlled temperature ($24 \pm 1^\circ\text{C}$) and 55% humidity with a 12-h light/dark cycle. Mice were raised with free access to food and water. After adaption for 1 week, mice were subcutaneously injected with 100 μl NCI-H460-CSC cells (2.5×10^6 cells), which were resuspended in ice-cold PBS. Subsequently, mice ($n=10$ in each group) were randomly assigned to three groups, including control, 400 and 800 mg/kg SchB groups. Mice in the control group were administered with PBS by oral gavage, while mice in the other two treatment groups were administered with 400 or 800 mg/kg SchB by oral gavage every day for 5 weeks. The size of tumors was measured at 1, 3, 7, 11, 14, 21, 28 and 35 days after cancer stem-like cell injection, and xenograft volume was calculated with the following formula: $\text{Volume} = \frac{1}{2} (L \times W^2)$. At the end of the experiment, neoplasms were removed and weighed after all mice were euthanized by CO_2 asphyxiation, at a flow rate of 30% volume displaced/minute (26).

Immunohistochemical (IHC) staining. Tumor tissues were fixed by 4% paraformaldehyde at 4°C for 72 h, and embedded in paraffin. Paraffin-embedded tumor samples were sliced into 5- μm -thick slides and subjected to heat pretreatment at 60°C for 1 h, followed by deparaffinization, and then rehydrated with xylene and a graded ethanol series. Following quenching using 3% hydrogen peroxide aqueous solution, sections were blocked with 10% goat serum (EMD Millipore) for 1 h at room temperature. Sections were incubated with a primary antibody for proliferating cell nuclear antigen (PCNA; Abcam; 1:500; cat. no. ab92552) at 4°C overnight, probed with HRP-conjugated secondary antibody (Abcam; 1:1,000; cat. no. ab6721) at 37°C for 30 min, treated with 3,3-diaminobenzidine and finally stained with hematoxylin at room temperature for 5 min. Sections were photographed under an inverted light microscope (Nikon Corporation; magnification, x100).

Immunofluorescence. Cancer stem-like cells (5×10^4 cells) were seeded on glass slides, immobilized in 4% formaldehyde at 4°C for 15 min, followed by permeation with 0.3% Triton X-100 and blocked using 10% goat serum (EMD Millipore) at room temperature for 30 min. Subsequently, slides were probed using an anti-p65 antibody (Abcam; 1:100; cat. no. ab32536) overnight at 4°C, incubated with rhodamine-labeled secondary antibody (Invitrogen; Thermo Fisher Scientific, Inc.; 1:350; cat. no. 31670) at room temperature for 1 h and stained with DAPI at room temperature for 5 min in the dark. Subsequently, the fluorescence signals were observed with a fluorescence microscope (BX61; Olympus Corporation; magnification, x400).

Statistical analysis. All statistical analyses were performed using SPSS 16 software (SPSS, Inc.). Results were presented as the mean \pm SD from three independent assays. Differences between 2 groups were analyzed by unpaired Student's t-test and differences among >2 groups were analyzed by one-way or two-way ANOVA with Tukey's correction. $P < 0.05$ was considered to indicate a statistically significant difference.

Results

SchB leads to toxicity in cancer stem-like cells derived from large-cell lung cancer cells. To establish cancer stem-like

cells, NCI-H460 and H661 cells were treated with serum-free DMEM/F12 medium containing the aforementioned growth factors. Considering that CD133⁺ cells exhibit stemness features, flow cytometry analysis was used for evaluation of CD133⁺ cells (27). Results in Fig. 1A demonstrated that the percentage of CD133⁺ cells in CSCs was significantly higher than that in parental cells (both $P < 0.01$; 8-fold increase of CD133⁺ cells in NCI-H460-CSCs and 13-fold increase in H661-CSCs compared with parental cells). To ensure the stemness of cancer stem-like cells, induced cells were also sorted and CD133⁺ cells were collected for subsequent experiments. In Fig. 1B, western blotting results indicated that the protein expression levels of CD44, Oct-4 and Bmi-1 were markedly upregulated in cancer stem-like cells compared with in the corresponding parental cells. Sphere-forming assay revealed that the number of spheres formed by NCI-H460-CSCs or H661-CSCs was increased by 30-fold compared with NCI-H460 or H661 cells, respectively, suggesting that induced cells had a stronger sphere-forming capacity compared with original cells (both $P < 0.01$; Fig. 1C). As represented in Fig. 1D, a marked increase in cells in the G₀/G₁ phase was observed in both NCI-H460-CSCs and H661-CSCs compared with their parental cells ($P < 0.01$). These findings indicated that the cancer stem-like cells used in the present study possessed a slower proliferation cycle compared with parental cells, due to cell cycle arrest at the G₀/G₁ phase. The aforementioned results proved that stemness of NCI-H460 and H661 cells was induced successfully. As a type of lignans widely used in Chinese medicine, SchB is an active extract from *Schisandra chinensis* Baill fruit and presents anticancer activities (Fig. 1E) (22). Therefore, the role of SchB was explored in large-cell lung cancer cell viability. It was observed that SchB treatment significantly decreased the viability of parental and cancer stem-like cells at concentrations $\geq 40 \mu\text{mol/l}$ ($P < 0.05$; Fig. 1F), indicating that administration of $\geq 40 \mu\text{mol/l}$ SchB caused cytotoxicity of cancer stem-like cells and parental cells.

SchB suppresses the migration, invasion and EMT of cancer stem-like cells. Subsequently, the effects of SchB on migration and invasion of cancer stem-like cells were investigated. Due to the cytotoxicity of SchB at concentrations $\geq 40 \mu\text{mol/l}$, cancer stem-like cells were treated with 10, 20 or 40 $\mu\text{mol/l}$ SchB for subsequent experiments. The wound healing assay revealed that the migratory ability of NCI-H460-CSCs was significantly decreased by 10–40 $\mu\text{mol/l}$ SchB treatment compared with the control group ($P < 0.05$ and $P < 0.01$), while the migratory ability of H661-CSCs was significantly decreased by 20–40 $\mu\text{mol/l}$ SchB treatment compared with the control group ($P < 0.01$; Fig. 2A). Similarly, significant repression of cell invasion was observed in SchB-treated cancer stem-like cells compared with in the control group ($P < 0.05$ and $P < 0.01$ for NCI-H460-CSCs, and $P < 0.01$ for H661-CSCs; Fig. 2B). Considering the important role of EMT in cell migration and invasion, alteration of EMT markers after SchB treatment was examined. Western blotting revealed that the administration of SchB caused upregulation of E-cadherin expression and downregulation of vimentin and N-cadherin expression in both NCI-H460-CSCs and H661-CSCs in a dose-dependent manner (Fig. 2C). Overall, these findings provided strong

evidence that SchB treatment impeded cancer stem-like cell migration, invasion and EMT.

SchB alleviates the stemness of cancer stem-like cells. Thereafter, the present study intended to assess the potential of SchB in CSC characteristics of NCI-H460-CSCs and H661-CSCs. As shown in Fig. 3A, the proportion of CD133⁺ cells in SchB-treated cancer stem-like cells was significantly lower than in the control group ($P < 0.05$ and $P < 0.01$ for H661-CSCs, and $P < 0.01$ for NCI-H460-CSCs). Similarly, western blotting data revealed that the protein expression levels of stem factors, including CD133, CD44, Oct-4 and Bmi-1, were markedly decreased in SchB-treated cells compared with in the control group (Fig. 3B). Furthermore, it was demonstrated by sphere-forming assay that administration of SchB significantly decreased the number of spheres compared with the control group (all $P < 0.01$; Fig. 3C). The current findings indicated that SchB exerted an inhibitory role in activities of cancer stem-like cells.

SchB results in the inhibition of the NF- κ B and p38 MAPK signaling pathways. In order to investigate the mechanism underlying SchB activity, the impact of SchB on key signaling pathways involved in tumor progression was assessed. The present results indicated that SchB significantly decreased the phosphorylation levels of I κ B α ($P < 0.01$) and p65 ($P < 0.05$ and $P < 0.01$ for NCI-H460-CSCs, and $P < 0.01$ for H661-CSCs) compared with the control group (Fig. 4A). Moreover, results of immunofluorescence staining assay suggested that SchB blocked p65 nuclear translocation (Fig. 4B). Subsequently, the expression levels of core proteins in the MAPK signaling pathway were detected by western blot analysis. It was revealed that SchB only significantly repressed the phosphorylation of p38 compared with the control ($P < 0.01$) in NCI-H460-CSCs and H661-CSCs, while there was no apparent change in phosphorylation levels of JNK and MEK in response to SchB treatment (Fig. 4C). Overall, SchB induced the inactivation of the NF- κ B and p38 MAPK signaling pathways.

SchB attenuates the CSC properties of NCI-H460-CSCs via regulation of the NF- κ B and p38 MAPK signaling pathways. To confirm the role of the NF- κ B and p38 MAPK signaling pathways in the tumor-suppressive properties of SchB, rescue experiments were performed. Considering the similar effects of SchB on NCI-H460-CSCs and H661-CSCs, rescue experiments were validated in NCI-H460-CSCs. The NF- κ B and p38 MAPK signaling pathways were activated via treatment with TNF- α and anisomycin, respectively. As demonstrated in Fig. 5A, TNF- α resulted in significantly enhanced phosphorylation levels of I κ B α and p65 compared with the control and SchB groups ($P < 0.01$), while SchB significantly dampened the TNF- α -mediated activation of the NF- κ B signaling pathway, showing a prominent decrease in phosphorylation levels of I κ B α and p65 compared with the TNF- α group ($P < 0.01$). Additionally, western blotting revealed that anisomycin significantly increased the phosphorylation of JNK, p38 and MEK compared with the control and SchB groups ($P < 0.01$; Fig. 5B). SchB treatment significantly decreased the anisomycin-mediated phosphorylation levels of p38 ($P < 0.01$), whereas it had no effects on JNK and MEK

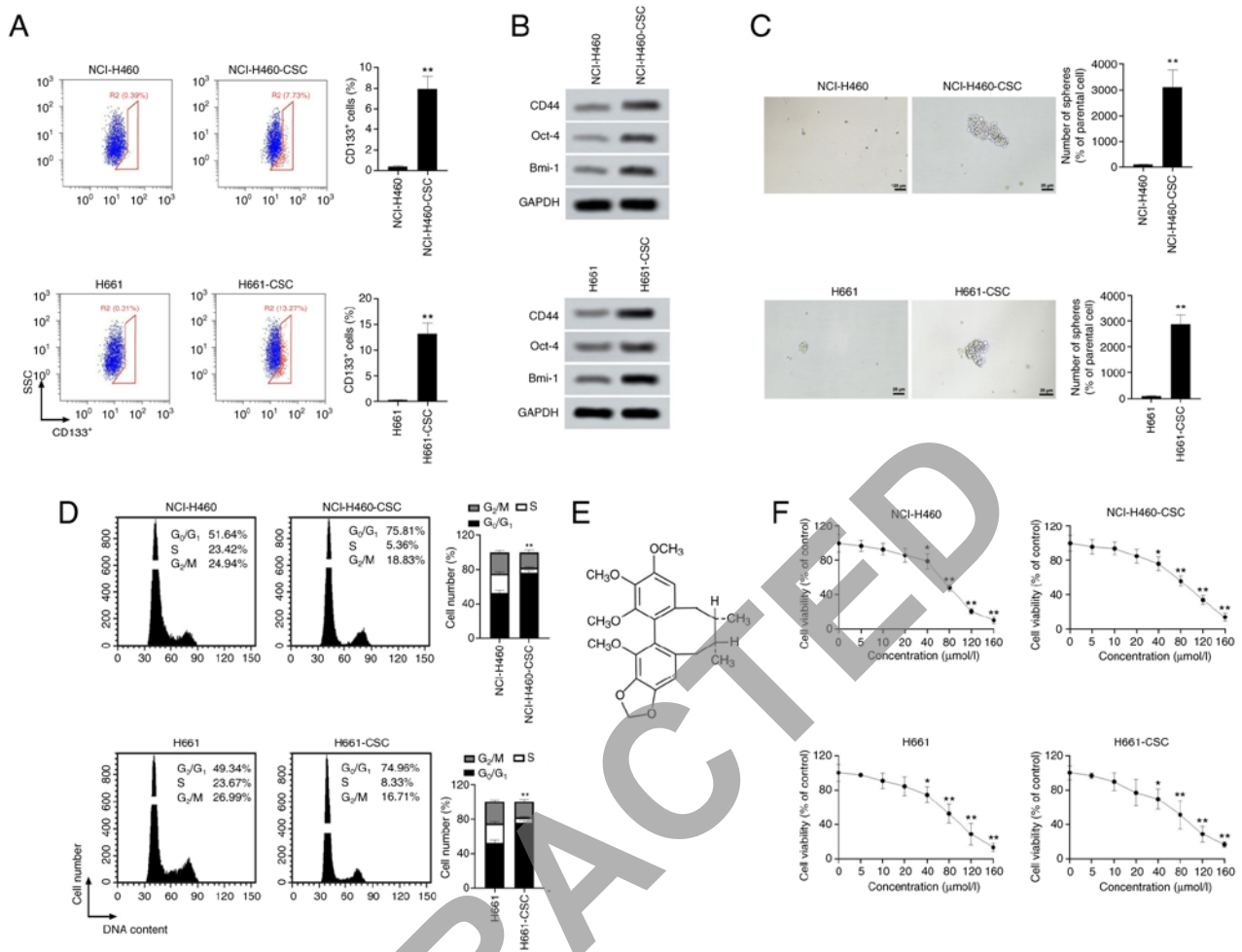


Figure 1. SchB leads to toxicity in cancer stem-like cells. To induce cancer stem-like cells, NCI-H460 and H661 cells were incubated in serum-free DMEM/F12 medium containing appropriate growth factors. (A) Following induction, the ratio of CD133⁺ cells was analyzed by flow cytometry. Blue cells represent CD133⁺ cells and red cells represent CD133⁻ cells. (B) Expression levels of CSC markers (CD44, Oct-4 and Bmi-1) were detected by western blot analysis. (C) Sphere-forming assay was performed to estimate CSC traits of large-cell lung cancer cells. Scale bar, 25 μ m. **P<0.01 vs. parental cells. (D) Cell cycle was evaluated by flow cytometry. **P<0.01 G₀/G₁ parental cells vs. cancer stem-like cells. (E) Chemical structure of SchB. (F) Cancer stem-like cells and parental cells were incubated with different doses of SchB (0, 5, 10, 20, 40, 80, 120 and 160 μ mol/l) for 72 h and Cell Counting Kit-8 assay was utilized to examine the viability of cancer stem-like cells and parental cells. Cells treated with 0 μ mol/l SchB acted as control. Differences were analyzed via one-way ANOVA with Tukey's correction. *P<0.05 and **P<0.01 vs. 0 μ mol/l. All experimental data are shown as the mean \pm SD (n=3). SSC, side scatter; SchB, Schisandrin B; CSC, cancer stem cell; Oct-4, octamer-binding transcription factor 4; Bmi-1, B lymphoma Mo-MLV insertion region 1 homolog.

phosphorylation (both P>0.05; Fig. 5B). Furthermore, it was observed that administration of SchB abolished the promotion of cell migration (Fig. 5C) and invasion (Fig. 5D) caused by TNF- α -induced NF- κ B signaling pathway activation and anisomycin-mediated p38 activation (all P<0.01). Moreover, the current findings validated that the impacts of TNF- α and anisomycin on the expression levels of EMT-associated proteins were significantly counteracted by SchB treatment (all P<0.01; Fig. 5E). The flow cytometry analysis indicated that SchB significantly decreased the elevated ratio of CD133⁺ cells induced by TNF- α or anisomycin (both P<0.01; Fig. 5F). Accordingly, activation of the NF- κ B and p38 MAPK signaling pathways upregulated the protein expression levels of CD133, CD44, Oct-4 and Bmi-1 in NCI-H460-CSCs, and their expression levels were restored by SchB treatment, as shown by significant decreases in protein expression levels (all P<0.01; Fig. 5G). The sphere-forming assay further confirmed that SchB significantly decreased the sphere-forming capability facilitated by TNF- α or anisomycin (both P<0.01;

Fig. 5H). Overall, SchB may exert an inhibitory role in the malignant behaviors of NCI-H460-CSCs by targeting the NF- κ B and p38 MAPK signaling pathways.

SchB restrains the growth and CSC characteristics of NCI-H460-CSCs in vivo. Based on the aforementioned results, the present study aimed to verify whether SchB had a tumor suppressor function in large-cell lung cancer *in vivo*. NCI-H460-CSCs were subcutaneously inoculated into nude mice, which were then administrated with 400 or 800 mg/kg SchB, with PBS used as a negative control. The size and weight of xenograft tumors were significantly repressed by SchB treatment compared with the control group (all P<0.01; Fig. 6A and B). PCNA encircles DNA and functions as a clamp for DNA polymerases, thus playing critical roles in numerous aspects of DNA replication and replication-associated processes (28). IHC assay revealed that SchB led to a marked decrease in PCNA expression in xenografts (Fig. 6C). Western blot analysis revealed that administration of SchB significantly

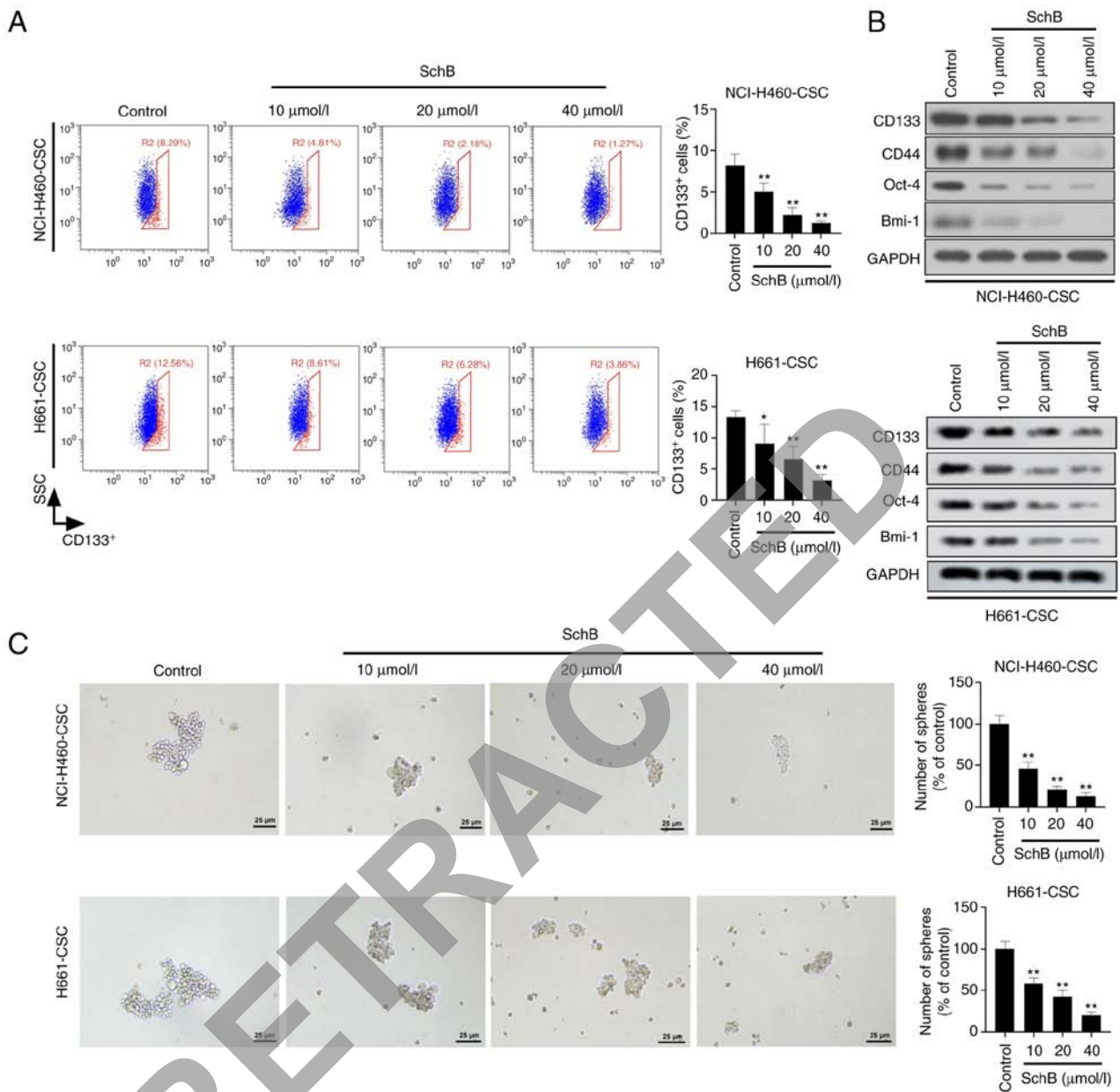


Figure 3. SchB alleviates the stemness of cancer stem-like cells. Cancer stem-like cells (NCI-H460-CSCs and H661-CSCs) were treated with 10, 20 or 40 $\mu\text{mol/l}$ SchB and the control group was treated with PBS. (A) Flow cytometry was used to evaluate the number of CD133⁺ cells. (B) CD133, CD44, Oct-4 and Bmi-1 expression was tested by western blot analysis. (C) Sphere-forming ability of cancer stem-like cells was estimated by sphere-forming assay. Scale bar, 25 μm . All experimental data are shown as the mean \pm SD (n=3). Differences were analyzed by one-way ANOVA with Tukey's correction. *P<0.05, **P<0.01 vs. control. SSC, side scatter; SchB, Schisandrin B; Oct-4, octamer-binding transcription factor 4; Bmi-1, B lymphoma Mo-MLV insertion region 1 homolog.

decreased the protein expression levels of CD133, CD44, Oct-4 and Bmi-1 compared with the control group (all P<0.01; Fig. 6E). Furthermore, SchB treatment significantly down-regulated p-I κ B α , p-p65 and p-p38 in neoplasms compared with the control group (P<0.05 or P<0.01; Fig. 6F). Therefore, the results indicated that SchB suppressed NCI-H460-CSC growth, EMT and stemness *in vivo*.

Discussion

The present study focused on the potentially tumor-suppressive role of SchB in large-cell lung cancer. NCI-H460 and H661 cells were used as protocells to induce CSCs. Notably, it was revealed that SchB suppressed migration, invasion, EMT

and stemness in CSCs. The NF- κ B and p38 MAPK signaling pathways were inactivated in SchB-treated cells, and effects of activating the NF- κ B or p38 MAPK signaling pathways were abolished by SchB. Effects of SchB on CSCs were also confirmed *in vivo*.

Mounting evidence has illustrated that CSCs serve an important part in the occurrence and development of tumors on account of their ability for self-renewal, differentiation and induction of tumor growth (29,30). Accordingly, large-cell lung cancer cells were stimulated with serum-free DMEM/F12 medium containing aforementioned growth factors to establish cancer stem-like cells in the present study. CD44, overexpressed in several types of cells, including CSCs, is involved in cell proliferation, differentiation and

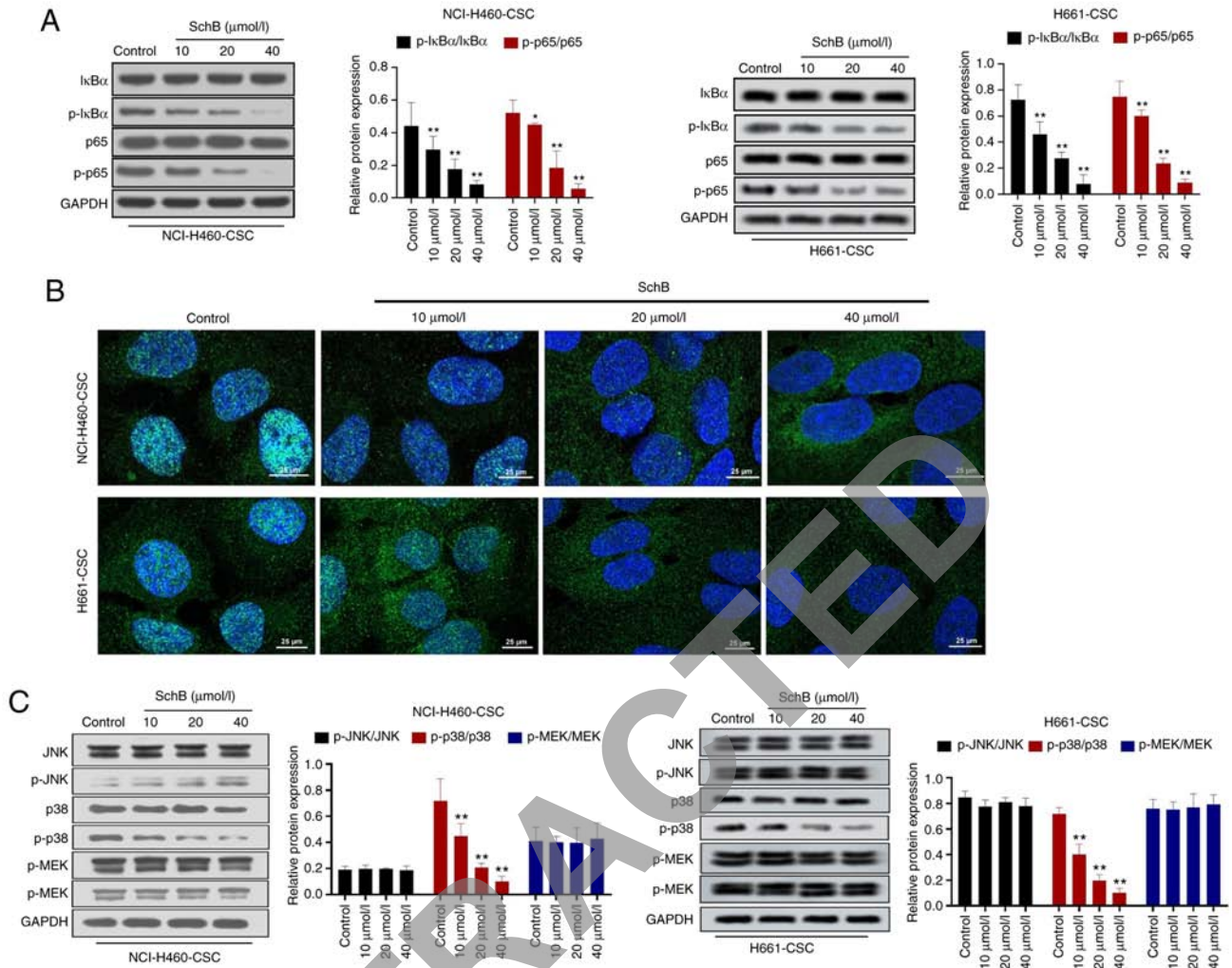


Figure 4. SchB results in the inhibition of the NF- κ B and p38 MAPK signaling pathways. Cancer stem-like cells (NCI-H460-CSCs and H661-CSCs) were treated with 10, 20 or 40 $\mu\text{mol/l}$ SchB and the control group was treated with PBS. (A) Protein expression levels of important genes in the NF- κ B signaling pathway (I κ B α and p65) were examined by western blot analysis. (B) Immunofluorescence assay was used to determine the nuclear translocation of p53 in cancer stem-like cells after SchB treatment. Scale bar, 25 μm . (C) Protein expression levels of JNK, p-JNK, p38, p-p38, MEK and p-MEK were measured by western blot analysis. Differences were analyzed by one-way ANOVA with Tukey's correction. * $P < 0.05$, ** $P < 0.01$ vs. control. SchB, Schisandrin B; I κ B α , inhibitor of nuclear factor κ B; p, phosphorylated.

migration (31). Oct-4 is also a CSC marker whose expression enhances features of CSCs (32). In addition, Bmi-1 behaves as a key regulator in the self-renewal, differentiation and tumor initiation and is thus widely used as a CSC marker (33). In addition to the proportion of CD133⁺ cells in induced cells and sphere formation of induced cells, the expression levels of CSC markers (CD44, Oct-4 and Bmi-1), as well as cell cycle, were detected in induced cells and protocells to confirm that cells used in the present study were CSCs and not a CSC-enriched population. Results revealed that both NCI-H460-CSCs and H661-CSCs presented stronger CSC traits compared with their parental cells.

The present findings revealed that SchB led to toxicity in both cancer stem-like cells and protocells at concentrations $\geq 40 \mu\text{mol/l}$. Cells were therefore treated with 10, 20 or 40 $\mu\text{mol/l}$ SchB in subsequent experiments to avert potential toxic effects of SchB on migration, invasion, EMT and stemness. Increasing studies have demonstrated that cell migration and EMT are associated with the features of cancer stem-like cells (34,35). Hence, the present study explored the effects of SchB on

cell migration, revealing that SchB restrained the migration, invasion and EMT of NCI-H460-CSCs and H661-CSCs. Furthermore, the detection results of stem markers indicated that SchB alleviated CSC characteristics of NCI-H460-CSCs and H661-CSCs. Previous studies have demonstrated that SchB exhibits a tumor suppressor function in multiple types of cancer, including glioma (36), gallbladder (37), gastric (38) and breast cancer (39). Consistently, the current data revealed the antitumor role of SchB in large-cell lung cancer cells.

As a transcription factor, NF- κ B is involved in regulating the expression levels of numerous crucial genes associated with apoptosis, inflammation, tumorigenesis and the progression of autoimmune diseases (40,41). Increasing evidence has indicated that the NF- κ B signaling pathway serves a key role in controlling EMT and CSC signatures of lung cancer cells (42,43). It is well documented that I κ B proteins are phosphorylated by the I κ B kinase complex and then nuclear translocation of NF- κ B enhances the activation of the NF- κ B signaling pathway, leading to tumor growth and the maintenance of stemness characteristics (44,45). In the current

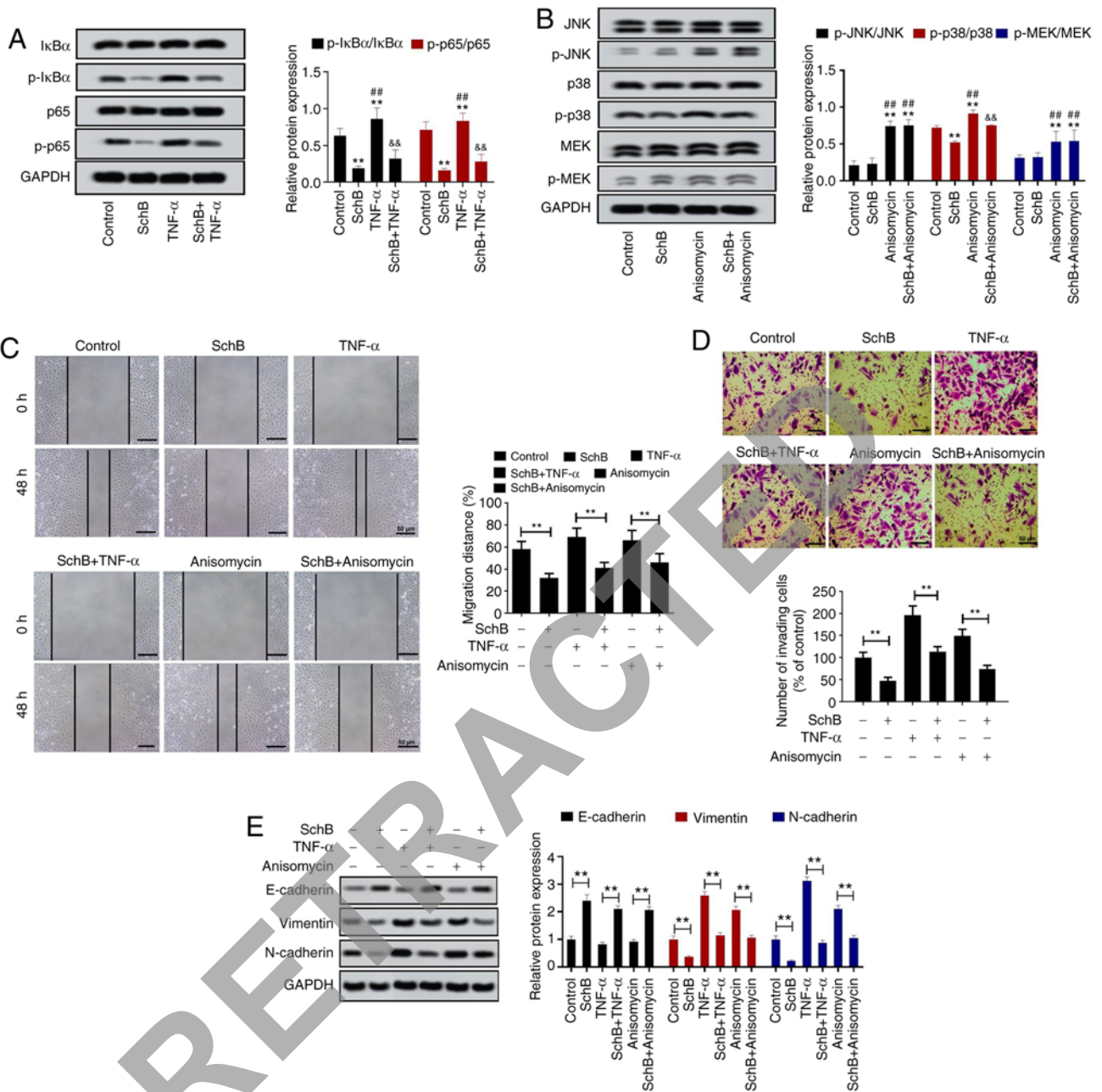


Figure 5. Continued.

study, it was revealed that SchB repressed the phosphorylation of IκBα and p65, as well as nuclear translocation of p65, indicating that SchB blunted the activation of the NF-κB signaling pathway in large-cell lung cancer. Additionally, the association between p38 MAPK and NF-κB activation has been confirmed in lung cancer cells (46). The p38 MAPK signaling pathway has been verified to regulate the NF-κB signaling pathway (47). Additionally, p38 functions as a facilitator in the transcriptional activity of NF-κB via mitogen- and stress-activated kinase 1-mediated p65 phosphorylation (48). A previous study has indicated that p38 MAPK contributes to the tumorigenesis and development of lung cancer (49). Therefore, the present study detected the impacts of SchB on key kinases (JNK, p38 and ERK) in the p38 MAPK signaling pathway, revealing that SchB only blocked the activation of p38 and had no significant effects on JNK and ERK.

In order to certify whether the functional role of SchB in large-cell lung cancer cells was mediated by the NF-κB and p38 MAPK signaling pathways, the activation of these pathways was induced using the corresponding pathway activators (TNF-α and anisomycin, respectively) and rescue experiments were performed. It was demonstrated that SchB abrogated the effects of NF-κB and p38 MAPK activation on large-cell lung cancer cell migration and invasion. Moreover, EMT and stemness features restrained by SchB were retrieved when NCI-H460-CSC cells were treated with TNF-α or anisomycin, further expounding the antitumor activities of SchB in large-cell lung cancer cells through repression of the NF-κB and p38 MAPK signaling pathways. In agreement with these results, animal assays indicated that SchB served as a tumor suppressor in the malignant phenotype of large-cell lung cancer *in vivo*. The toxicity of a drug is a pivotal inspection

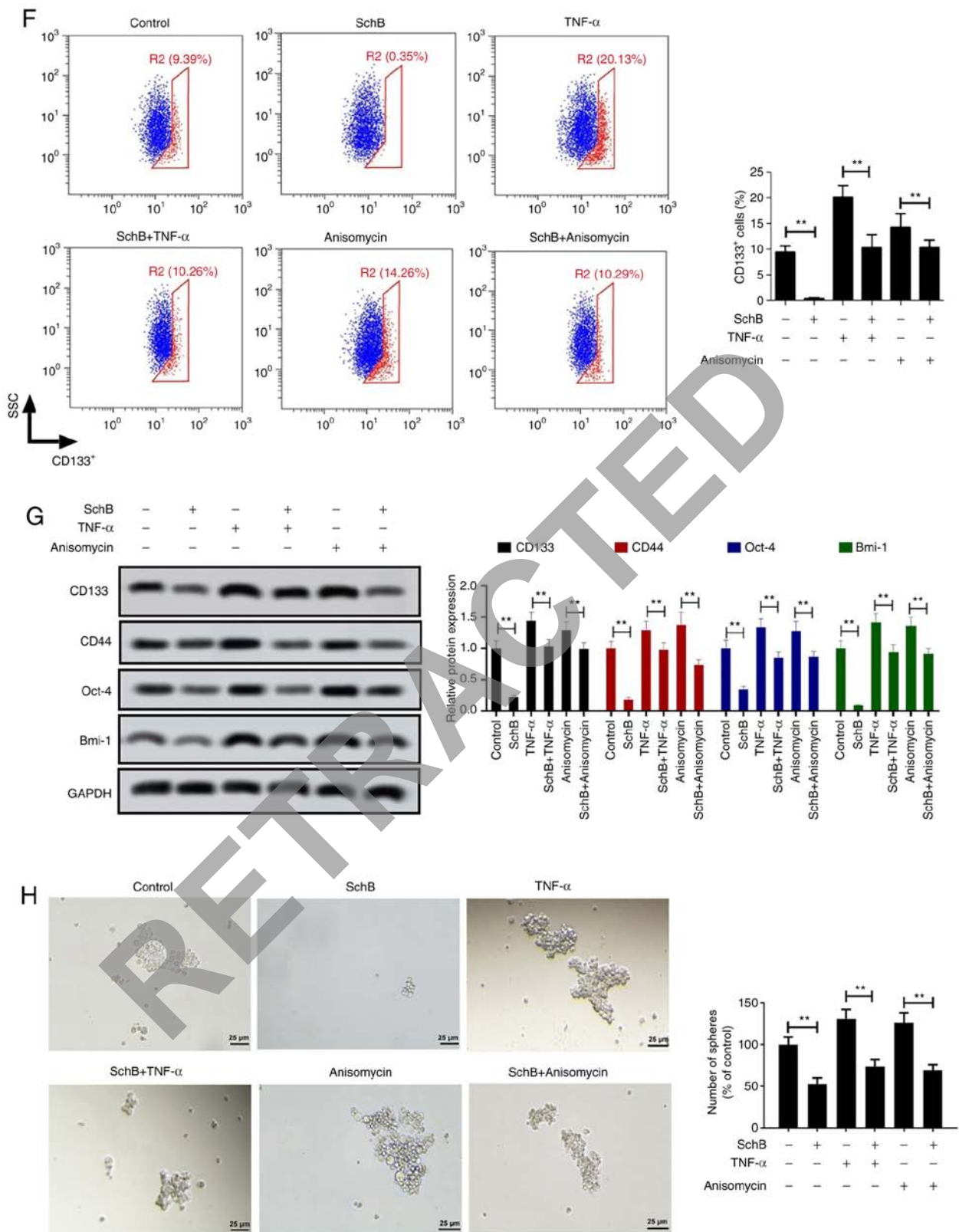


Figure 5. SchB attenuates the CSC properties of NCI-H460-CSCs via regulation of the NF- κ B and p38 MAPK signaling pathways. To explore the role of the NF- κ B and p38 MAPK signaling pathways in the effects of SchB on large-cell lung cancer, NCI-H460-CSCs were treated with 40 μ mol/l SchB for 12 h and then stimulated with 10 ng/ml TNF- α or 2 ng/ml anisomycin for 30 min. Cells administrated with PBS or SchB alone were used as controls. Western blot was implemented to detect the expression levels of associated proteins in the (A) NF- κ B and (B) MAPK signaling pathways. Differences were analyzed via two-way ANOVA with Tukey's correction. ** P <0.01 vs. control. ## P <0.01 vs. SchB. &#P<0.01 TNF- α /anisomycin. (C) Cell migration and (D) invasion were assessed by wound healing and Transwell assays, respectively. Scale bar, 50 μ m. (E) Expression levels of EMT-associated proteins were examined by western blot analysis. (F) Proportion of CD133⁺ cells was analyzed by flow cytometry. Blue cells represent CD133⁻ cells and red cells represent CD133⁺ cells. (G) Protein expression levels of CD133, CD44, Oct-4 and Bmi-1 were determined by western blot analysis. (H) Sphere-forming assay was used to evaluate stemness in NCI-H460-CSCs. Scale bar, 25 μ m. All experimental data are shown as the mean \pm SD (n =3). *** P <0.01. SSC, side scatter; SchB, Schisandrin B; CSC, cancer stem cell; Oct-4, octamer-binding transcription factor 4; Bmi-1, B lymphoma Mo-MLV insertion region 1 homolog; I κ B α , inhibitor of nuclear factor κ B α ; p, phosphorylated.

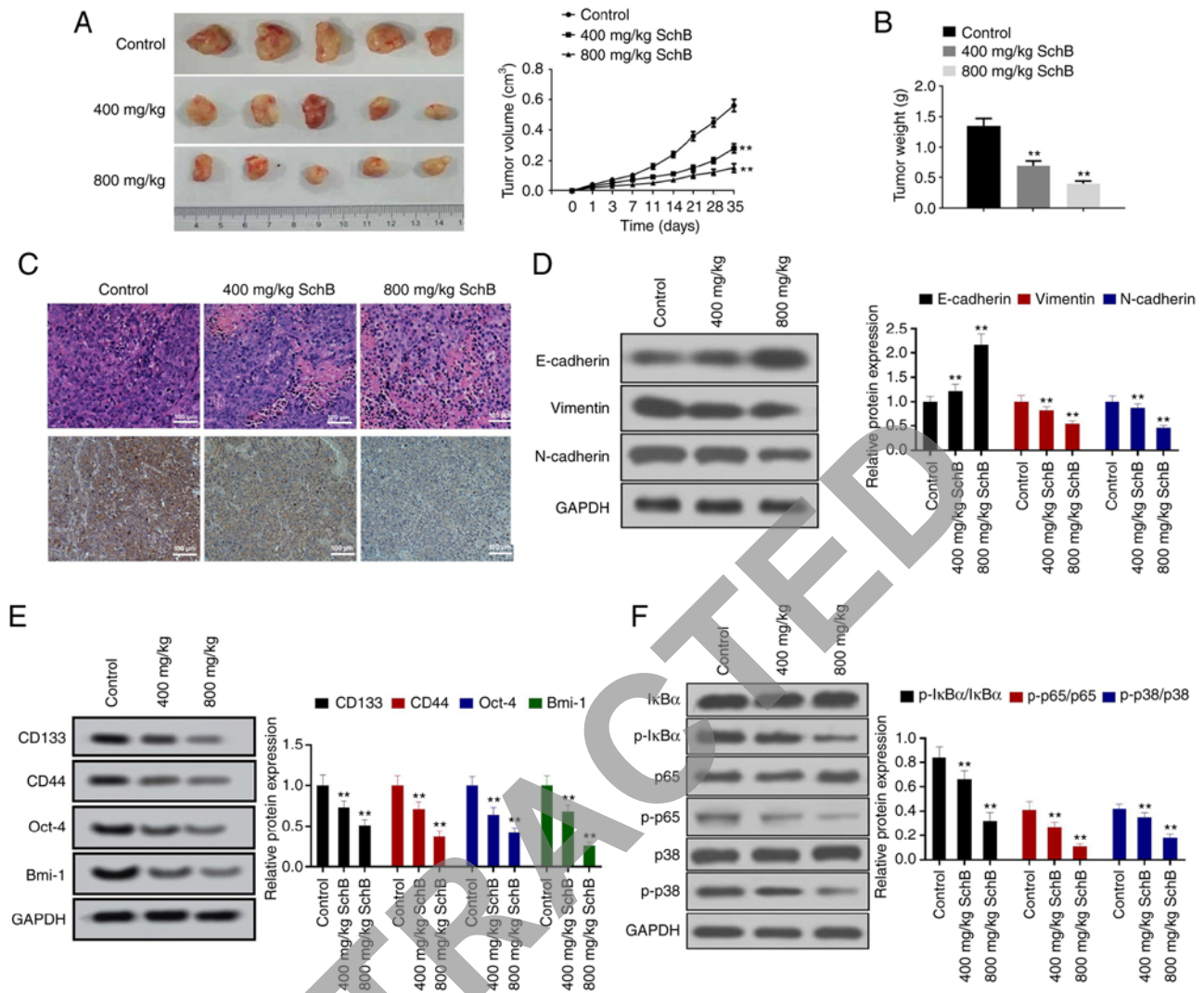


Figure 6. SchB restrains the growth and CSC characteristics of NCI-H460-CSCs *in vivo*. Nude mice were divided into three groups: Control, 400 mg/kg SchB and 800 mg/kg SchB groups. After subcutaneous injection with NCI-H460-CSCs, mice in the SchB-treated groups were administrated with 400 or 800 mg/kg SchB by oral gavage and mice treated with PBS were used as a negative control. (A) Size and (B) weight of neoplasms isolated from mice in different groups. (C) Hematoxylin and eosin, and immunohistochemical analyses for proliferating cell nuclear antigen in tumor tissues. Scale bar, 100 μ m. Western blotting was conducted to estimate the impact of SchB on (D) EMT, (E) stemness and (F) NF- κ B and p38 MAPK signaling pathways. All experimental data are shown as the mean \pm SD (n=10). Differences were analyzed by one-way ANOVA with Tukey's correction. **P<0.01 vs. control. SchB, Schisandrin B; CSC, cancer stem cell; Oct-4, octamer-binding transcription factor 4; Bmi-1, B lymphoma Mo-MLV insertion region 1 homolog; I κ B α , inhibitor of nuclear factor κ B α ; p, phosphorylated.

index for its potential application in the clinic. In previous *in vivo* experiments, mice implanted with triple-negative breast cancer cells were injected with 50 or 100 mg/kg SchB intraperitoneally once per day; no significant changes in body weight were noted in any of the experimental groups (22). In another study by Kwan *et al* (50), neither administration of a single dose of SchB at 800 mg/kg nor administration of SchB at 50 mg/kg/day for 14 consecutive days exhibited significant diminution in body weight in high-fat-diet-fed mice. Nevertheless, further studies are required to fully verify the safety of SchB prior to clinical usage.

To the best of our knowledge, the present study was the first to clarify the role and molecular mechanism of SchB in EMT and stemness traits of large-cell lung cancer cells. It was demonstrated that SchB suppressed cell migration, invasion, EMT and CSC properties in large-cell lung cancer via regulation of the NF- κ B and p38 MAPK signaling pathways.

However, the specific regulatory mechanism underlying SchB in the inactivation of the NF- κ B and p38 MAPK signaling pathways, and the association between these pathways remain unclear. Additionally, other EMT-associated signaling pathways, such as SMAD, PI3K/AKT, Wnt and Notch, may also participate in the SchB-involved regulation, and should be further investigated in future studies. The potential difference of tumorigenesis between cancer stem-like cells and parental cells is also a topic that requires further exploration. Overall, the present findings confirmed the anticancer function of SchB in cancer stem-like cells, revealing that SchB may be used as a promising drug for the treatment of large-cell lung cancer.

Acknowledgements

Not applicable.

Funding

No funding was received.

Availability of data and materials

All data generated or analyzed during this study are included in this published article.

Authors' contributions

HW, LW and RM designed the study. SL completed all the assays. SL and LW assessed all the raw data to ensure its legitimacy, and conducted data analyses. SL and LW were responsible for writing the manuscript. All authors read and approved the final manuscript, and are responsible for confirming the authenticity of the data.

Ethics approval and consent to participate

All experimental animal procedures performed in the present study were approved by the Ethics Committee of the First Affiliated Hospital of Chengdu Medical College (Chengdu, China; approval no. SCXK 2018-19).

Patient consent for publication

Not applicable.

Competing interests

The authors declare that they have no competing interests.

References

- Bray F, Ferlay J, Soerjomataram I, Siegel RL, Torre LA and Jemal A: Global cancer statistics 2018: GLOBOCAN estimates of incidence and mortality worldwide for 36 cancers in 185 countries. *CA Cancer J Clin* 68: 394-424, 2018.
- Jemal A, Bray F, Center MM, Ferlay J, Ward E and Forman D: Global cancer statistics. *CA Cancer J Clin* 61: 69-90, 2011.
- Guo T, Kong J, Liu Y, Li Z, Xia J, Zhang Y, Zhao S, Li F, Li J and Gu C: Transcriptional activation of NANOG by YBX1 promotes lung cancer stem-like properties and metastasis. *Biochem Biophys Res Commun* 487: 153-159, 2017.
- Hirsch FR, Scagliotti GV, Mulshine JL, Kwon R, Curran WJ Jr, Wu YL, Wu YL and Paz-Ares L: Lung cancer: Current therapies and new targeted treatments. *Lancet* 389: 299-311, 2017.
- Wang K, Gong Q, Zhan Y, Chen B, Yin T, Lu Y, Zhang Y, Wang H, Ke J, Du B, *et al.*: Blockage of autophagic flux and induction of mitochondria fragmentation by paroxetine hydrochloride in lung cancer cells promotes apoptosis via the ROS-MAPK pathway. *Front Cell Dev Biol* 7: 397, 2019.
- Lathia JD and Liu H: Overview of cancer stem cells and stemness for community oncologists. *Target Oncol* 12: 387-399, 2017.
- Valent P, Bonnet D, De Maria R, Lapidot T, Copland M, Melo JV, Chomienne C, Ishikawa F, Schuringa JJ, Stassi G, *et al.*: Cancer stem cell definitions and terminology: The devil is in the details. *Nat Rev Cancer* 12: 767-775, 2012.
- Visvader JE and Lindeman GJ: Cancer stem cells in solid tumours: Accumulating evidence and unresolved questions. *Nat Rev Cancer* 8: 755-768, 2008.
- Lapidot T, Sirard C, Vormoor J, Murdoch B, Hoang T, Caceres-Cortes J, Minden M, Paterson B, Caligiuri MA and Dick JE: A cell initiating human acute myeloid leukaemia after transplantation into SCID mice. *Nature* 367: 645-648, 1994.
- Ponti D, Costa A, Zaffaroni N, Pratesi G, Petrangolini G, Coradini D, Pilotti S, Pierotti MA and Daidone MG: Isolation and in vitro propagation of tumorigenic breast cancer cells with stem/progenitor cell properties. *Cancer Res* 65: 5506-5511, 2005.
- Magee JA, Piskounova E and Morrison SJ: Cancer stem cells: Impact, heterogeneity, and uncertainty. *Cancer Cell* 21: 283-296, 2012.
- Yue Y, Xia L, Xu S, Wang C, Wang X, Lu W and Xie X: SURF4 maintains stem-like properties via BIRC3 in ovarian cancer cells. *J Gynecol Oncol* 31: e46, 2020.
- Jimenez-Hernandez LE, Vazquez-Santillan K, Castro-Oropeza R, Martinez-Ruiz G, Muñoz-Galindo L, Gonzalez-Torres C, Cortes-Gonzalez CC, Victoria-Acosta G, Melendez-Zajgla J and Maldonado V: NRP1-Positive lung cancer cells possess tumor-initiating properties. *Oncol Rep* 39: 349-357, 2018.
- Yang S, Chen T, Huang L, Xu S, Cao Z, Zhang S, Xu J, Li Y, Yue Y, Lu W, *et al.*: High-Risk human papillomavirus E7 maintains stemness via APH1B in cervical cancer stem-cell like cells. *Cancer Manag Res* 11: 9541-9552, 2019.
- Davis FM, Stewart TA, Thompson EW and Monteith GR: Targeting EMT in cancer: Opportunities for pharmacological intervention. *Trends Pharmacol Sci* 35: 479-488, 2014.
- Dongre A and Weinberg RA: New insights into the mechanisms of epithelial-mesenchymal transition and implications for cancer. *Nat Rev Mol Cell Biol* 20: 69-84, 2019.
- Abu-Elheiga L, Jayakumar A, Baldini A, Chirala SS and Wakil SJ: Human acetyl-CoA carboxylase: Characterization, molecular cloning, and evidence for two isoforms. *Proc Natl Acad Sci USA* 92: 4011-4015, 1995.
- Mani SA, Guo W, Liao MJ, Eaton EN, Ayyanan A, Zhou AY, Zhou AY, Brooks M, Reinhard F, Zhang CC, *et al.*: The epithelial-mesenchymal transition generates cells with properties of stem cells. *Cell* 133: 704-715, 2008.
- Liu GT: Pharmacological actions and clinical use of fructus schizandrae. *Chin Med J (Engl)* 102: 740-749, 1989.
- Lee MY, Seo CS, Lee NH, Ha H, Lee JA, Lee H, Lee Ky and Shin HK: Anti-Asthmatic effect of schizandrin on OVA-induced airway inflammation in a murine asthma model. *Int Immunopharmacol* 10: 1374-1379, 2010.
- Nasser MI, Han T, Adlat S, Tian Y and Jiang N: Inhibitory effects of schizandrin B on human prostate cancer cells. *Oncol Rep* 41: 677-685, 2019.
- Dai X, Yin C, Guo G, Zhang Y, Zhao C, Qian J, Wang O, Zhang X and Liang G: Schizandrin B exhibits potent anticancer activity in triple negative breast cancer by inhibiting STAT3. *Toxicol Appl Pharmacol* 358: 110-119, 2018.
- Jiang Y, Zhang Q, Bao J, Du C, Wang J, Tong Q, Liu C: Schizandrin B inhibits the proliferation and invasion of glioma cells by regulating the HOTAIR-miRNA-125a-mTOR pathway. *Neuroreport* 28: 93-100, 2017.
- Lv XJ, Zhao LJ, Hao YQ, Su ZZ, Li JY, Du YW and Zhang J: Schizandrin B inhibits the proliferation of human lung adenocarcinoma A549 cells by inducing cycle arrest and apoptosis. *Int J Clin Exp Med* 8: 6926-6936, 2015.
- Zhuang W, Li Z, Dong X, Zhao N, Liu Y, Wang C and Chen J: Schizandrin B inhibits TGF- β 1-induced epithelial-mesenchymal transition in human A549 cells through epigenetic silencing of ZEB1. *Exp Lung Res* 45: 157-166, 2019.
- Li H, Meng X, Zhang D, Xu X, Li S and Li Y: Ginkgolic acid suppresses the invasion of HepG2 cells via downregulation of HGF/c-met signaling. *Oncol Rep* 41: 369-376, 2019.
- Suresh R, Ali S, Ahmad A, Philip PA and Sarkar FH: The role of cancer stem cells in recurrent and drug-resistant lung cancer. *Adv Exp Med Biol* 890: 57-74, 2016.
- Kang MS, Ryu E, Lee SW, Park J, Ha NY, Ra JS, Kim YJ, Kim J, Abdel-Rahman M, Park SH, *et al.*: Regulation of PCNA cycling on replicating DNA by RFC and RFC-like complexes. *Nat Commun* 10: 2420, 2019.
- Capp JP: Cancer stem cells: From historical roots to a new perspective. *J Oncol* 2019: 5189232, 2019.
- Najafi M, Farhood B and Mortezaee K: Cancer stem cells (CSCs) in cancer progression and therapy. *J Cell Physiol* 234: 8381-8395, 2019.
- Chen C, Zhao S, Karnad A and Freeman JW: The biology and role of CD44 in cancer progression: Therapeutic implications. *J Hematol Oncol* 11: 64, 2018.
- Wang D, Lu P, Zhang H, Luo M, Zhang X, Wei X, Gao J, Zhao Z and Liu C: Oct-4 and nanog promote the epithelial-mesenchymal transition of breast cancer stem cells and are associated with poor prognosis in breast cancer patients. *Oncotarget* 5: 10803-10815, 2014.

33. Althobiti M, Muftah AA, Aleskandarany MA, Joseph C, Toss MS, Green A and Rakha E: The prognostic significance of BMI1 expression in invasive breast cancer is dependent on its molecular subtypes. *Breast Cancer Res Treat* 182: 581-589, 2020.
34. McCoy MG, Nyanyo D, Hung CK, Goerger JP, Zipfel WR, Williams RM, Nishimura N and Fischbach C: Endothelial cells promote 3D invasion of GBM by IL-8-dependent induction of cancer stem cell properties. *Sci Rep* 9: 9069, 2019.
35. Wang F, Ma L, Zhang Z, Liu X, Gao H, Zhuang Y, Yang P, Kornmann M, Tian X and Yang Y: Hedgehog signaling regulates epithelial-mesenchymal transition in pancreatic cancer stem-like cells. *J Cancer* 7: 408-417, 2016.
36. Jiang Y, Zhang Q, Bao J, Du C, Wang J, Tong Q and Liu C: Schisandrin B suppresses glioma cell metastasis mediated by inhibition of mTOR/MMP-9 signal pathway. *Biomed Pharmacother* 74: 77-82, 2015.
37. Xiang SS, Wang XA, Li HF, Shu YJ, Bao RF, Zhang F, Cao Y, Ye YY, Weng H and Wu WG: Schisandrin B induces apoptosis and cell cycle arrest of gallbladder cancer cells. *Molecules* 19: 13235-13250, 2014.
38. Liu XN, Zhang CY, Jin XD, Li YZ, Zheng XZ and Li L: Inhibitory effect of schisandrin B on gastric cancer cells in vitro. *World J Gastroenterol* 13: 6506-6511, 2007.
39. Liu Z, Zhang B, Liu K, Ding Z and Hu X: Schisandrin B attenuates cancer invasion and metastasis via inhibiting epithelial-mesenchymal transition. *PLoS One* 7: e40480, 2012.
40. Liu B, Cao W and Ma H: Knockdown of lncRNA LSINCT5 suppresses growth and metastasis of human glioma cells via up-regulating miR-451. *Artif Cells Nanomed Biotechnol* 47: 2507-2515, 2019.
41. Serramito-Gomez I, Boada-Romero E, Slowicka K, Vereecke L, Van Loo G and Pimentel-Muñoz FX: The anti-inflammatory protein TNFAIP3/A20 binds the WD40 domain of ATG16L1 to control the autophagic response, NFKB/NF-kappaB activation and intestinal homeostasis. *Autophagy* 15: 1657-1659, 2019.
42. Kumar M, Allison DF, Baranova NN, Wamsley JJ, Katz AJ, Bekiranov S, Bekiranov S, Jones DR and Mayo MW: NF-κB regulates mesenchymal transition for the induction of non-small cell lung cancer initiating cells. *PLoS One* 8: e68597, 2013.
43. Murayama T, Nakaoku T, Enari M, Nishimura T, Tominaga K, Nakata A, Tojo A, Sugano S, Kohno T and Gotoh N: Oncogenic fusion gene CD74-NRG1 confers cancer stem cell-like properties in lung cancer through a IGF2 autocrine/paracrine circuit. *Cancer Res* 76: 974, 2016.
44. Zakaria N, Yusoff NM, Zakaria Z, Widera D and Yahaya BH: Inhibition of NF-κB signaling reduces the stemness characteristics of lung cancer stem cells. *Front Oncol* 8: 166, 2018.
45. Perkins ND: Integrating cell-signalling pathways with NF-kappaB and IKK function. *Nat Rev Mol Cell Biol* 8: 49-62, 2007.
46. Hsieh KY, Wei CK and Wu CC: YC-1 prevents tumor-associated tissue factor expression and procoagulant activity in hypoxic conditions by inhibiting p38/NF-κB signaling pathway. *Int J Mol Sci* 20: 244, 2019.
47. Li T, Wu YN, Wang H, Ma JY, Zhai SS and Duan J: Dapk1 improves inflammation, oxidative stress and autophagy in LPS-induced acute lung injury via p38MAPK/NF-κB signaling pathway. *Mol Immunol* 120: 13-22, 2020.
48. Ghosh S and Hayden MS: New regulators of NF-κB in inflammation. *Nat Rev Immunol* 8: 837-848, 2008.
49. Tian X, Wang Y, Li S, Yue W and Tian H: ZHX2 inhibits proliferation and promotes apoptosis of human lung cancer cells through targeting p38MAPK pathway. *Cancer Biomark* 27: 75-84, 2020.
50. Kwan HY, Niu X, Dai W, Tong T, Chao X, Su T, Chan CL, Lee KC, Fu X, Yi H and Yu H: Lipidomic-Based investigation into the regulatory effect of schisandrin B on palmitic acid level in non-alcoholic steatotic livers. *Sci Rep* 5: 9114, 2015.



This work is licensed under a Creative Commons Attribution-NonCommercial-NoDerivatives 4.0 International (CC BY-NC-ND 4.0) License.

RETRACTED